

Light Olefins Production in a Fixed Bed Reactor Using Alumina Supported Iron-Cobalt-Cerium Oxide Nanocatalysts Prepared by Impregnation Procedure: Effect of Preparation Conditions on Nanocatalyst Performance

Ali Akbar Mirzaei ¹ , Behdokht Hashemi Hosseini ¹ , Sajjad Porgar ^{2,*} 

¹ Department of Chemistry, Faculty of Sciences, University of Sistan and Baluchestan, Zahedan, Iran; Behdokht.hashemi.hosseini@gmail.com (B.H.H.);

² Department of Chemical Engineering, South Tehran Branch, Islamic Azad University, Tehran, Iran; sajjad.porgar@gmail.com (S.P.);

* Correspondence: sajjad.porgar@gmail.com;

Scopus Author ID 57202874495

Received: 15.11.2020; Revised: 9.12.2020; Accepted: 10.12.2020; Published: 13.12.2020

Abstract: In this study, pretreatment conditions such as impregnation time and temperature and drying time and temperature for the production of the iron-cobalt-cerium catalyst with impregnation method as a first step for controlling the synthesis of a new type of three similar metal phase ratio were determined by the Taguchi method. A microtubular fixed bed reactor tested the catalysts' performance under constant conditions according to conversion. The activity and selectivity toward propylene and ethylene have been calculated. The catalyst, which impregnated at 90 °C for 4hr and dried at 120 °C for 24hr, had the best catalytic performance. According to previous studies, the catalyst calcined and the reactor test was performed in the constant and optimum condition such as calcinations in 600 °C for 6hr, reduction with H₂ (flow = 30 mL.min⁻¹) for 90 min and P~1atm and also the reaction terms was H₂:CO = 1 (flow H₂ = 37.5 mL.min⁻¹ and CO = 37.5 mL.min⁻¹) and p=1bar. Finally, The characterization was done by XRD, SEM, BET, and test on the precursor, optimized catalyst, and optimized catalyst after reactor tests, which all were showed the nanosized catalyst particles.

Keywords: Fischer-Tropsch synthesis; nanocatalyst; catalyst characterization; wet impregnation method; iron-cobalt-cerium catalyst.

© 2020 by the authors. This article is an open-access article distributed under the terms and conditions of the Creative Commons Attribution (CC BY) license (<https://creativecommons.org/licenses/by/4.0/>).

1. Introduction

Fischer-Tropsch Synthesis as a source of good quality liquid fuels, in recent years, it has devoted a large part of the technical, economic, and industrial studies and scientific research to major oil companies [1, 2]. At present, fuel and chemical production is based on crude oil. Since methane and coal are much more than crude oil, natural gas and methane can be converted to fuel and chemicals from effective saving, cost, and environmental benefits. To be this process can be very useful in four directions. First, it is one way to convert gas into a liquid that makes transporting easier; secondly, it directly generates portable hydrocarbon-based fuels; the third advantage is that the hydrocarbon fuels they produce are excellent quality. This means that there are very few environmental pollutants and other impurities such as aromatics, sulfur, nitrogen compounds, and heavy metals [3,4]. Therefore the fuels derived from this

process are referred to as clean fuels. Ultimately the storage of expired resources Oil and its rising cost will make the Fischer Tropsch process more noticeable [3,5,6] and try to improve that day by day. Fischer Tropsch Synthesis is part of the important process of GTL, in which synthesis gas (mainly containing H₂ and CO from coal, natural gas, or natural gas) is converted into a mixture of hydrocarbons. Changes influence this in the catalyst composition, feed H₂/CO ratio, temperature, pressure, and reactor type. In addition to hydrocarbons, other beneficial chemicals may also be produced, increasing or decreasing the amount of these materials by varying ratios and conditions. Most of the products of the Fischer Trout Process are hydrocarbon fuels (gasoline, diesel fuel, and jet), olefins, waxes, and oxygenates (such as alcohols) [7, 8].

2. Materials and Methods

2.1. Reactions in Fischer-Tropsch synthesis.

These reactions can be divided into three categories:

- The main reactions are paraffin and olefins [9, 10].



Reactions (1) and (2) for the production of paraffin and reactions (3) and (4) for the production of olefins. Another reaction, which is a major reaction, is the reaction of gas displacement.



- Side reactions, which are the product of alcohols, are also the reaction of Boudouard (7) in this category. This reaction leads to the formation of coke at the catalyst level and reduces catalytic activity.



- Catalytic changes, which include the reduction of catalyst oxidation, the formation of metal carbide in the production of catalysts, which is well seen in the latter case in the production of iron.



2.2. Catalytic preparation steps.

This section will discuss the operations that should be done on the primary catalyst, including [2, 11]: Rinsing; Filtering; Drying; Forming; Calcinations.

2.3. Rinsing.

The impurities can be removed with the help of a rinse operation. This will continue to continue until the concentration of undesirable species is reduced to a minimum. Washing is not necessary for catalysts produced by inoculation, and catalysts produced in a coordinating

manner sometimes have a pH stabilizing factor with undesirable species that need to be removed. For example, sodium ions in the catalyst can be caused by sodium hydrogen carbonate, sodium carbonate can be title acts as an intrinsic poisoning agent, and even other species that sometimes play the promoter's role must be optimally optimized, so most materials require this action for catalyst precursors. The washing operation has the following goals: Harmful substances are removed from the inside of the catalyst. The water is in the space between the particles instead of the mother solution and the inert molecules; In the washing operation, the water dissolves ions that remain at the solid surface in sedimentation; Exchange some unwanted or unwanted ions by other ions that can easily be decanted by calcination.

2.4. Filtering.

Catalysts for filtering in the laboratory can be used Buchner funnel and paper strainers, but commercially available using industrial filter filters.

2.5. Drying.

There are various drying methods, including drying in the oven at atmospheric pressure and drying fine droplets of vacuum solvent pre-vacuum solvent, including these methods. Drying can be carried out at a temperature between 100 and 600 °C [12-14]. Depending on the catalyst's structure and characteristics, the variable's temperature is usually between 100 and 150°C. The drying time can also be an effective factor in how the catalyst works, depending on the type of structure and the catalyst characteristics. The drying temperature can be in different ranges, which can usually range from 4h. If the drying rate is high, the high velocity of evaporation in the pores will disrupt the catalyst. However, using the test method and the error at different velocities and temperatures and checking the final catalyst's quality, it is possible to dry using the mathematical model optimally.

2.6. Forming.

After drying, depending on the test conditions, the particles' size can be determined by sieving the meshes in one of these ways. It can also occasionally be obtained by peeling or extruding, which usually comes with the receptor (for binding) and softening agents (for ease of forming into powder).

2.7. Calcinations.

Technically, the calcining and drying processes are similar. The difference is that drying is carried out at temperatures in the range of 150-1050 °C. However, calcinations sometimes occur at temperatures above 1000 °C. In the process of calcining, the chemical and physical properties of the material change, by doing so, not only the size of the pores but also their distribution. By increasing the calcinations temperature, a clear difference in the pore diameter is created. As a result, the total volume of the pores and their area significantly decreases, one of which is the growth of the growth of the crystals forming the catalyst. In practice, the airflow's calcinations from the catalyst with the gradual increase of temperature pass through until the temperature reaches its maximum. Calcining is very important for the following reasons: Loss of crystalline water molecules, i.e., water molecules that have been bonded with metal atoms, do not get out of the catalyst structure during the drying process due

to the bond's strength; Exit of unnecessary materials such as binders, lubricants, esophagus, and unstable anions and cations such as chlorine, NO₃, NH₃, and CO₂; Changes in the distribution of pore size in the catalyst structure; Catalyst reaches the best form in terms of stability, structure, and active phase formation; Achieving mechanical stability; Scattering of metal action and forming it in proper design and structure Sample resuscitation [15].

In the recovery phase, the resulting oxides are streams of hydrogen or a mixture of hydrogen with another gas. The temperature and purity of the reducing agent are important factors in the process of reducing metal oxides. By changing the percentage of the metal present in the catalyst structure or changing the process temperature, it is possible to control their distribution, for example, in iron-based catalysts, with the increase in the temperature of resuscitation of the surface, the surface, the volume of catalyst cavities is reduced and its activity decreases. Cobalt, nickel, and ruthenium are almost always reduced to H₂ at temperatures between 473- 723 K and remain under metallic conditions under reaction conditions.

Fischer-Tropsch Synthesis activity and selectivity on Co/C catalysts and its reaction condition has been studied in Table 1.

Table 1. Reaction Condition on Fischer-Tropsch Synthesis.

Ref.	Catalyst	T (°C)	GHSV	CO%
[16]	Co/C	220	3600	9,22,38
[17]	ZIF-67	500	5550	60
[18]	Co-BDC	550	3000	10.5
[19]	CPO-27(Co)	500	2800	1.1
[20]	ZIF-67	600	6.75	34.2
[21]	MOF-1	500	3600	65.1
[22]	25%Co/N-NGC	220	-	86.9
[23]	6.1%Co/carbon spheres	232	-	21
[24]	15%Co-3wt.%Cr/AC	220	-	45.6
[25]	10%Co/N-HCS	220	-	34
[26]	20%Co-0.1%Pt/NaBEA	250	-	63

Many other researchers are also have done in the field of Fischer -Tropsch [27-31].

2.8. Optimal catalyst preparation method.

The nanocatalyst in this study was made of three metals, iron (Fe), cobalt (CO), cerium (Ce), by inoculation method. In this method, three half-molar solutions of the metal nitrates CO(NO₃)₂.6H₂O, Fe (NO₃)₃.9H₂O, Ce(NO₃)₂.6H₂O and then another solution containing an equal ratio of metals. The materials were purchased from Merck factory with purity above 97% that is summarized in Table 2.

Table 2. Material used in the synthesis of catalysts.

Molecular weight	Purity (%)	manufacturing factory	Chemical substance
404	98	MERCK	Fe(NO ₃) ₃ .9H ₂ O
291.04	97	MERCK	Co(NO ₃) ₂ .6H ₂ O
434	98.5	MERCK	Ce (NO ₃) ₂ .6H ₂ O
191	99	MERCK	Al ₂ O ₃

We add a certain amount of solution to 5% by weight (based on the weight of metals), powdered alumina (calcined at 600 °C for 6 h), and the resulting mixture at different temperatures from 30 to 90 °C over time 4-8 hr is inoculated in Rotary. Then we straighten it with a Buchner funnel. The precipitate is dried at various temperatures of 90 °C for a period 6-24 h, called a precursor. 9 precursors are made, as shown in Table 3.

The resulting precursors were calcined for 6 h at 600 °C, and final catalysts were obtained. The optimum catalytic catalyst was dried at 90 °C for 4 hours for 24 hours in an autoclave with a temperature of 120 °C.

Table 3. Synthesized catalysts.

Drying temperature (°C)	Drying time (h)	Inoculation temperature (°C)	Inoculation time(h)	Catalyst
90	6	60	4	1
90	24	30	6	2
150	6	90	6	3
150	15	30	4	4
120	15	60	6	5
120	24	90	4	6
120	6	30	8	7
150	24	60	8	8
90	15	90	8	9

Table 4. Analysis of the XRD precursor spectrum, optimal catalyst, and catalyst after testing

h.K.l	Nano size	Number	Space group	Constant network	Crystalline species	Compound name	Reference code	Type
012	25.5575	13	P-3M1	a=5.036A° b=5/0360A° c=13/7720A° α=90° β=90° δ=90°	Orthorhombic	FeHO ₂	010770247	Precursor
012	28.0584	17	R-3	a=5/0360A° b=5/0360A° c=13/7720A° α=90° β=90° δ=120°	Rhombohedral	Fe ₂ O ₃	00240072	Catalyst
220	29.8343	15	Pm3m	a=2/81A° b=2/81A° c=2/81A° α=90° β=90° δ=90°	Cubic	Fe ₂ Si	000261141	After the test of the reactor

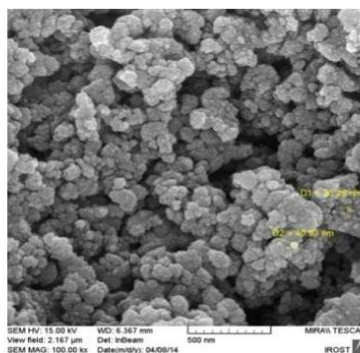
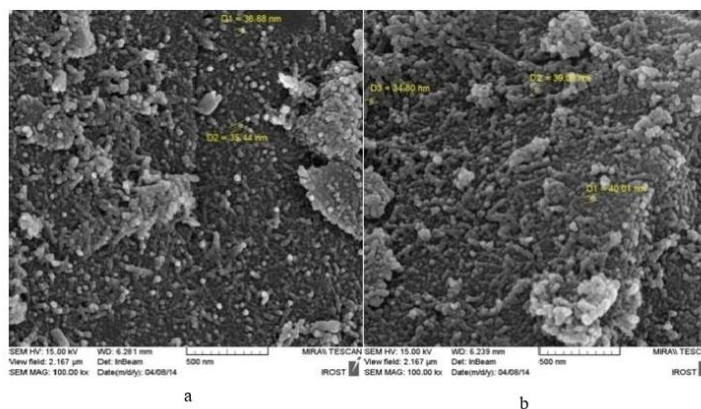


Figure 1. a) the precursor, (b) an optimal catalyst, and (c) a catalyst after SEM test.

The shape, size, and distribution of crystals are important structural features. This method is an appropriate tool for morphology. The separation problems limit this technique to investigate crystals larger than 5nm. SEM investigations on many systems have been carried out to identify crystals and studies on the structure of cavities. The SEM machine sample with VEGA/TASCAN model, which is available at Tehran Polymer and Petrochemical Institute, is used. Table 4 presents the XRD results and also gives information about the catalyst.

The comparison of Figures 1.a, 1.b, and 1.c show that the precursor has continuous, dense, and coarse particles. However, during the calcinations process, these particles become smaller and smaller due to the formation of new phases and the release of volatile organic compounds. However, for the catalyst after the test, due to the formation of carbide phases, the catalytic cracking and resuscitation phenomenon is somewhat larger.

Using the BET method, the optimal catalyst area, precursor, and catalyst after the test was examined. The results are presented in Table 5.

Table 5. BET results (m^2/g).

Catalyst (after testing)	Optimal catalyst	Precursor
90.1120	137.6620	97.9299

The catalysts produced, the calcite catalysts, have a greater surface area than the precursor due to the outflow of water in the precursor that creates a cavity and increases the surface area. Carefully, in the results, it is noted that the catalysts have a slight decrease in surface area after the test, which is due to the filling of catalyst cavities during catalytic operations. The carbide phases in the catalyst after the test indicate the filling of the cavities by the carbides.

2.9. Laboratory unit reactor test.

The device's overall work is to mix synthetic gases removed from the capsules with the desired rate and then react to them and then provide the desired solution. Figure 2 shows the schematic of the apparatus that is used in this research.

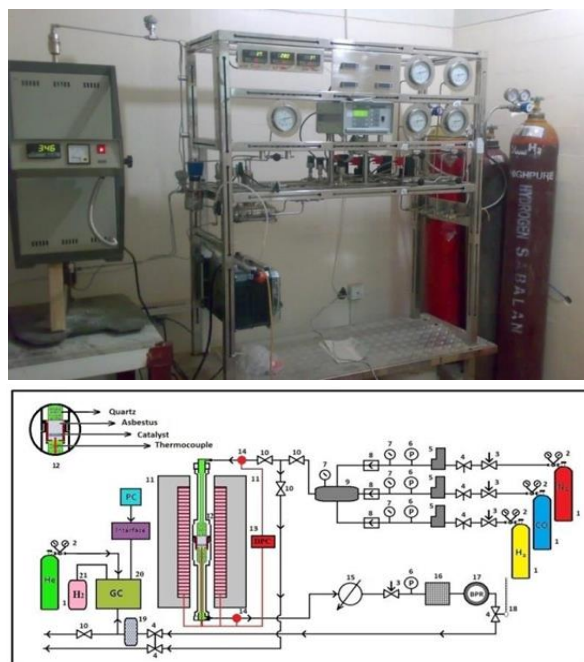


Figure 2. Schematic of the used micro-reactor study of catalytic activity and performance evaluation of catalysts.

In this section, the conditions for temperature and time of inoculation, temperature and drying time, temperature and recovery time, and calcification and constant spatial velocity were discussed to test the reactor, respectively. As discussed in the previous section (technical notes), the conventional procedure after catalyst construction is to resuscitate the catalyst and test the catalyst in a small reactor and examine its performance on a small scale. Creating a catalyst and changing the inoculation temperature and inoculation time, as well as temperature and drying time, are effective factors; therefore, different conditions were made in nine modes, not the catalyst and the pivotal difference. The catalyst was prepared by inoculation at different inoculation temperature (30, 60, 90 °C) and different inoculation periods (4,6 and 8 hr) and different drying temperatures (90,120,150°C) in the duration of time (6,15,24 hr) was developed by Taguchi experimental design method and showed in Table 6.

Table 6. Factors and test levels determined by the Taguchi experimental design.

Third level	Second level	First level	Parameters
90	60	30	Inoculation temperature (°C)
8	6	4	Inoculation time (hr)
150	120	90	Drying temperature (°C)
24	15	6	Drying time (hr)

The reaction conditions including the resuscitation temperature of 400 °C by hydrogen for 3hr and 30 ml/min, and the reaction temperature of 350 °C with flux 37.5 ml/min hydrogen and CO at H₂/CO = 1, and the calcinations temperature of 600°C for 6 hr and GHSV=4500 hr⁻¹ were considered the same for all types of catalysts. The results for each catalyst are listed in the optimal catalyst table. The catalyst is chosen as the best catalyst, with the highest CO conversion rate and selectivity for the desired products, while also having the least selectivity for the methane product. Tables 7 and 8, present the catalytic resuscitation conditions and operation conditions, respectively.

Table 7. Catalytic resuscitation conditions by H₂.

Pressure(bar)	Flux (mL.min ⁻¹)	Temperature(°C)	Time(hr)
~1	30	400	3

Table 8. Conditions for performing a test of a reactor.

Space velocity(hr ⁻¹)	Pressure(bar)	Flux (mL.min ⁻¹)	Temperature(°C)	Time(hr)
4500	1	H ₂ =37.5 CO=37.5	350	1.5

3. Results and Discussion

3.1. Operating conditions of catalysts.

According to each computational chromatogram, according to the formulas, numbers were obtained for each product's selectivity and yield. Optimal products are ethylene and propylene, so ethylene and propylene are considered a good products, and methane is considered undesirable. Other products are identified as (RT). Another point is that the number (RT) is related to how many gas chromatography outputs are. The absence of ethylene or propylene, or both in the tables, means that they are not produced.

In this section, we performed the test steps to obtain the necessary data to optimize temperature and time of inoculation, temperature and drying time. The final Table 9 was obtained after the calculations on the data obtained from the test of the nine catalysts. There are two common methods, one considering the number of experiments with the highest

selectivity for desired products such as ethylene and propylene, the activity, and the best catalyst's lowest methane production. The results of the activity of products are presented in Figure 3.

Table 9. Optimize temperature and time of inoculation, temperature and drying time

Cat. No	COin	CO out	Methane	Ethylene	Propylene	Conversion	sel. Meth	sel. Ethyl.	sel. propyl.	Y Meth.	Y ethyl.	Y propyl.
1	5274001	506480	38231	-	-	3.966628	0.18274	-	-	26.4382	-	-
2	5274001	4935496	684507	9202	10014	6.418372	2.02214	0.02718	0.02958	85.1932	1.14527	1.24633
3	5274001	5005571	25519	20797	-	5.089684	0.09506	0.07747	-	12.9630	10.5644	-
4	5274001	4803351	24866	1107	-	8.923965	0.05283	0.00235	-	3.05975	0.13621	-
5	5274001	5025586	636360	5640	29779	4.710181	2.56168	0.02270	0.11987	11.9521	0.10593	0.55931
6	5274001	5006850	113591	1780109	22329	5.065433	4.25195	66.6330	0.08358	2.77949	43.5579	0.05463
7	5274001	4951066	795087	15355	24824	6.12315	2.46206	0.04754	0.07687	44.8121	0.86542	1.39911
8	5274001	4879077	684500	57897	146740	7.488129	1.73324	0.14660	0.37156	34.8686	2.97319	7.53557
9	5274001	5136379	634832	8889	9236	2.609442	4.61286	0.06459	0.06711	85.2830	1.19414	1.24076

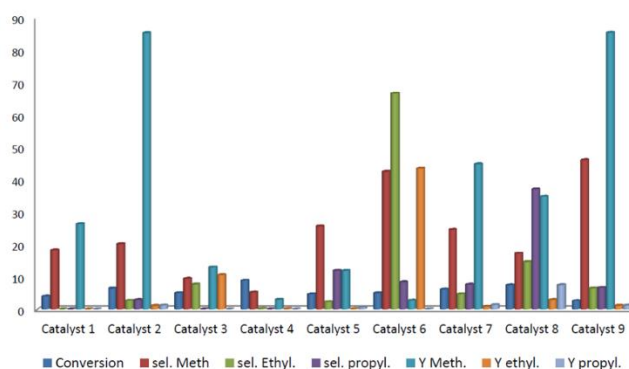


Figure 3. Distribution of selectivity and efficiency (activity) of products from reaction with catalysts.

3.2. XRD results.

The precursors of this catalyst are completely amorphous. The identified phases for calcined catalysts are a mixture of iron oxides, cobalt, and cerium before the reactor test. The phases identified for XRD tests after the test are often carbide and metal phases.

3.3. BET results.

All of the precursors have a higher surface area than the calcined catalyst before and after the reactor's test due to the outflow of water in the precursor, which in this place is a hole and increases the surface area. After the test, the calcined catalyst shows a slight decrease in surface area than the pre-test specimen due to the mooring.

3.4. Results from SEM.

The particle tissue in the precursor and the calcined sample is very different. The particle size in the calcined catalyst is smaller due to the degradation during the calcinations process.

The SEM comparison of the calcined sample before and after the reactor test also shows that the catalyst test has a significant effect on the catalyst's texture and structure, which can be attributed to the formation of metal and carbide phases.

4. Conclusions

The purpose of this research is to obtain an optimal catalyst for inoculums temperatures and inoculums times, as well as the best temperatures and drying times made by wet inoculation. Identification tests included XRD, SEM, BET on the calcined catalyst. The approximate size of the catalyst particle is less than 100 nm in terms of the XRD spectrum. Two important operations were performed to reduce the mass transfer effects. First, the nanoparticle catalyst reduced the edges and corners. The spatial speed of GHSV = 4500 hr⁻¹ was chosen, which could affect the reaction speed and penetration of the hole.

Experiments were carried out at different drying and inoculation temperatures for different periods and to prepare the optimal catalyst for the reactor's test on 9 different catalysts. Finally, the best catalyst obtained was catalyzed at 90 °C for 4 hours, inoculated at 120 °C dried for 24 hours, and showed the best performance. It should be noted that all of the catalysts were calcified at 600°C for 6hr. The resuscitation temperature was 400 °C for 3 hr, and the hydrogen gas discharge for 30mL/min and P = 1atm were the same for all of them.

Funding

This research received no external funding.

Acknowledgments

This research has no acknowledgment.

Conflicts of Interest

The authors declare no conflict of interest.

References

1. Aasberg-Petersen, K. *Studies in Surface Science and Catalysis*. Elsevier Science, **2004**; pp. 258-405.
2. Gurbani, A.; Ayastuy, J.L.; González-Marcos, M.P.; Herrero, J.E.; Guil, J.M.; Gutiérrez-Ortiz, M.A. Comparative study of CuO–CeO₂ catalysts prepared by wet impregnation and deposition–precipitation. *International Journal of Hydrogen Energy* **2009**, *34*, 547-553, <https://doi.org/10.1016/j.ijhydene.2008.10.047>.
3. Schulz, H. Short history and present trends of Fischer–Tropsch synthesis. *Applied Catalysis A: General* **1999**, *186*, 3-12, [https://doi.org/10.1016/S0926-860X\(99\)00160-X](https://doi.org/10.1016/S0926-860X(99)00160-X).
4. Demirbas, A. Combustion Efficiency Impacts of Biofuels. *Energy Sources, Part A: Recovery, Utilization, and Environmental Effects* **2009**, *31*, 602-609, <https://doi.org/10.1080/15567030701743718>.
5. Tavakoli, A.; Sohrabi, M.; Kargari, A. Application of Anderson–Schulz–Flory (ASF) equation in the product distribution of slurry phase FT synthesis with nanosized iron catalysts. *Chemical Engineering Journal* **2008**, *136*, 358-363, <https://doi.org/10.1016/j.cej.2007.04.017>.
6. Takeshita, T.; Yamaji, K. Important roles of Fischer–Tropsch synfuels in the global energy future. *Energy Policy* **2008**, *36*, 2773-2784, <https://doi.org/10.1016/j.enpol.2008.02.044>.
7. Marano, J.J. *Options for Upgrading & Refining Fischer-Tropsch Liquids*. 2nd International Freiberg Conference on IGCC & Xtl Technologies: Freiberg, Germany. **2007**.
8. Raje, A.; Inga, J.R.; Davis, B.H. Fischer-Tropsch synthesis: Process considerations based on performance of iron-based catalysts. *Fuel* **1997**, *76*, 273-280, [https://doi.org/10.1016/S0016-2361\(96\)00185-8](https://doi.org/10.1016/S0016-2361(96)00185-8).
9. Dry, M.E. Fischer–Tropsch reactions and the environment. *Applied Catalysis A: General* **1999**, *189*, 185-190, [https://doi.org/10.1016/S0926-860X\(99\)00275-6](https://doi.org/10.1016/S0926-860X(99)00275-6).
10. Dalmon, J.A.; Martin, G.A. The kinetics and mechanism of carbon monoxide methanation over silica-supported nickel catalysts. *Journal of Catalysis* **1983**, *84*, 45-54, [https://doi.org/10.1016/0021-9517\(83\)90084-2](https://doi.org/10.1016/0021-9517(83)90084-2).
11. Vásquez, P.G.; Cáceres, C.V.; Blanco, M.N.; Thomas, H.J. Prediction of concentration profiles in alumina spheres impregnated with molybdenum solutions. *International Communications in Heat and Mass Transfer* **1989**, *16*, 581-591, [https://doi.org/10.1016/0735-1933\(89\)90061-4](https://doi.org/10.1016/0735-1933(89)90061-4).

12. Bilbao-Sáinz, C.; Andrés, A.; Fito, P. Hydration kinetics of dried apple as affected by drying conditions. *Journal of Food Engineering* **2005**, *68*, 369-376, <https://doi.org/10.1016/j.jfoodeng.2004.06.012>.
13. Arsalanfar, M.; Mirzaei, A.A.; Bozorgzadeh, H.R.; Atashi, H.; Shahriari, S.; Pourdolat, A. Structural characteristics of supported cobalt–cerium oxide catalysts used in Fischer–Tropsch synthesis. *Journal of Natural Gas Science and Engineering* **2012**, *9*, 119-129, <https://doi.org/10.1016/j.jngse.2012.05.015>.
14. Mirzaei, A.A.; Arsalanfar, M.; Bozorgzadeh, H.R.; Samimi, A.J.P.C.R. A review of Fischer-Tropsch synthesis on the cobalt based catalysts. *Physical Chemistry Research* **2014**, *2*, 179-201, <https://dx.doi.org/10.22036/pcr.2014.5786>.
15. Aluha, J; Yongfeng, H.N.A. *Catalysts* **2017**, 1–19.
16. Luo, Q.-X.; Guo, L.-P.; Yao, S.-Y.; Bao, J.; Liu, Z.-T.; Liu, Z.-W. Cobalt nanoparticles confined in carbon matrix for probing the size dependence in Fischer-Tropsch synthesis. *Journal of Catalysis* **2019**, *369*, 143-156, <https://doi.org/10.1016/j.jcat.2018.11.002>.
17. Li, N.; Ma, C.-P.; Zhang, C.-H.; Yang, Y.; Li, Y.-W. Low-cost preparation of carbon-supported cobalt catalysts from MOFs and their performance in CO hydrogenation. *Journal of Fuel Chemistry and Technology* **2019**, *47*, 428-437, [https://doi.org/10.1016/S1872-5813\(19\)30020-9](https://doi.org/10.1016/S1872-5813(19)30020-9).
18. Rivera-Torrente, M.; Hernández Mejía, C.; Hartman, T.; de Jong, K.P.; Weckhuysen, B.M. Impact of Niobium in the Metal–Organic Framework-Mediated Synthesis of Co-Based Catalysts for Synthesis Gas Conversion. *Catalysis Letters* **2019**, *149*, 3279-3286, <https://doi.org/10.1007/s10562-019-02899-0>.
19. Chen, Y.; Li, X.; Nisa, M.U.; Lv, J.; Li, Z. ZIF-67 as precursor to prepare high loading and dispersion catalysts for Fischer-Tropsch synthesis: Particle size effect. *Fuel* **2019**, *241*, 802-812, <https://doi.org/10.1016/j.fuel.2018.12.085>.
20. Janani, H.; Mirzaei, A.A.; Rezvani, A. Correlation of metal–organic framework structures and catalytic performance in Fischer–Tropsch synthesis process. *Reaction Kinetics, Mechanisms and Catalysis* **2019**, *128*, 205-215, <https://doi.org/10.1007/s11144-019-01626-5>.
21. Taghavi, S.; Tavasoli, A.; Asghari, A.; Signoretto, M. Loading and promoter effects on the performance of nitrogen functionalized graphene nanosheets supported cobalt Fischer-Tropsch synthesis catalysts. *International Journal of Hydrogen Energy* **2019**, *44*, 10604-10615, <https://doi.org/10.1016/j.ijhydene.2019.03.015>.
22. Kuang, T.; Lyu, S.; Liu, S.; Zhang, Y.; Li, J.; Wang, G.; Wang, L. Controlled synthesis of cobalt nanocrystals on the carbon spheres for enhancing Fischer–Tropsch synthesis performance. *Journal of Energy Chemistry* **2019**, *33*, 67-73, <https://doi.org/10.1016/j.jechem.2018.08.012>.
23. Zhao, Z.; Lu, W.; Feng, C.; Chen, X.; Zhu, H.; Yang, R.; Dong, W.; Zhao, M.; Lyu, Y.; Liu, T.; Jiang, Z.; Ding, Y. Increasing the activity and selectivity of Co-based FTS catalysts supported by carbon materials for direct synthesis of clean fuels by the addition of chromium. *Journal of Catalysis* **2019**, *370*, 251-264, <https://doi.org/10.1016/j.jcat.2018.12.022>.
24. Dlamini, M.W.; Phaahlamohlaka, T.N.; Kumi, D.O.; Forbes, R.; Jewell, L.L.; Coville, N.J. Post doped nitrogen-decorated hollow carbon spheres as a support for Co Fischer-Tropsch catalysts. *Catalysis Today* **2020**, *342*, 99-110, <https://doi.org/10.1016/j.cattod.2019.01.070>.
25. Flores, C.; Batalha, N.; Marcilio, N.R.; Ordonsky, V.V.; Khodakov, A.Y. Influence of Impregnation and Ion Exchange Sequence on Metal Localization, Acidity and Catalytic Performance of Cobalt BEA Zeolite Catalysts in Fischer-Tropsch Synthesis. *ChemCatChem* **2019**, *11*, 568-574, <https://doi.org/10.1002/cctc.201800728>.
26. Gavrilović, L.; Save, J.; Blekkan, E.A. The Effect of Potassium on Cobalt-Based Fischer–Tropsch Catalysts with Different Cobalt Particle Sizes. *Catalysts* **2019**, *9*, <https://doi.org/10.3390/catal9040351>.
27. [Dai, Y.; Zhao, Y.; Lin, T.; Li, S.; Yu, F.; An, Y.; Wang, X.; Xiao, K.; Sun, F.; Jiang, Z.; Lu, Y.; Wang, H.; Zhong, L.; Sun, Y. Particle Size Effects of Cobalt Carbide for Fischer–Tropsch to Olefins. *ACS Catalysis* **2019**, *9*, 798-809, <https://doi.org/10.1021/acscatal.8b03631>.
28. Guo, S.; Wang, Q.; Wang, M.; Ma, Z.; Wang, J.; Hou, B.; Chen, C.; Xia, M.; Jia, L.; Li, D. A comprehensive insight into the role of barium in catalytic performance of Co/Al₂O₃ catalyst for Fischer-Tropsch synthesis. *Fuel* **2019**, *256*, <https://doi.org/10.1016/j.fuel.2019.115911>.
29. Tian, Z.; Wang, C.; Yue, J.; Zhang, X.; Ma, L. Effect of a potassium promoter on the Fischer–Tropsch synthesis of light olefins over iron carbide catalysts encapsulated in graphene-like carbon. *Catalysis Science & Technology* **2019**, *9*, 2728-2741, <https://doi.org/10.1039/c9cy00403c>.
30. Becker, H.; Güttel, R.; Turek, T. Performance of diffusion-optimised Fischer–Tropsch catalyst layers in microchannel reactors at integral operation. *Catalysis Science & Technology* **2019**, *9*, 2180-2195, <https://doi.org/10.1039/c9cy00457b>.